LBL-18508
September 1985
To Be Published In
Energy and Buildings

DAYLIGHTING SIMULATION IN THE DOE-2 BUILDING ENERGY ANALYSIS PROGRAM

Frederick Winkelmann and Stephen Selkowitz

Energy Efficient Buildings Program
Applied Science Division
Lawrence Berkeley Laboratory
University of California
Berkeley, California 94720

ABSTRACT

A daylighting calculation has been integrated into the DOE-2 building energy analysis computer program. Users can, for the first time in a widely-accepted, publicly-available program, determine the impact of daylight utilization on heating and cooling loads, energy use, energy cost, and peak electrical demand. We describe the algorithms which simulate hourly-varying interior illuminance, management of windows for sun and glare control, and the operation of electric lighting control systems. Sample DOE-2 daylighting output reports are presented and results of program validation against scale model illuminance measurements using the Lawrence Berkeley Laboratory sky simulator are discussed.

1. INTRODUCTION

Use of natural lighting can be a cost-effective way to reduce electrical energy consumption and, at the same time, enhance the quality of the indoor environment. For several years, architects and engineers have used scale models, hand calculator programs, and sophisticated mainframe computer programs to determine levels of interior daylight for different building configurations. However, none of these tools determines the impact of daylighting on overall energy use and peak electrical loads, information which could have an important effect on design decisions. For this reason, a daylighting simulation has been added to the DOE-2 building energy use analysis program. This model, in conjunction with the DOE-2 thermal loads and HVAC analysis [1,2], determines the energy- and cost-related consequences of daylighting strategies based upon hour-by-hour analysis of daylight availability, site conditions, window management in response to solar gain and glare, and various lighting control strategies.

The daylighting simulation which is described in the following sections has three main stages:

(1) Daylight factor preprocessor: By integrating transmitted luminous flux over the area of each window (or skylight), interior illuminance at user-selected room locations is calculated for a standard overcast sky and for clear sky conditions with 20 different sun positions. Dividing the interior illuminance by the corresponding exterior illuminance gives daylight factors which are stored for later interpolation in the hourly simulation. The interior illuminance calculation accounts for the luminance distribution of the sky; window size, slope and orientation; glass transmittance; inside surface reflectances; sun control devices such as drapes and overhangs; and external obstructions. Analagous factors for the discomfort glare from each window are also calculated for each sun and sky condition and stored.

(2) Hourly daylighting simulation: The hourly illuminance and glare contribution from each window is found by interpolating the stored daylight factors using the current-hour sun position and cloud cover, then multiplying by the current-hour exterior horizontal illuminance. If the glare-control option has been specified, the program automatically closes window blinds or drapes in order to decrease glare below a pre-defined comfort level. A similar option uses window shading devices to automatically control solar gain.

This procedure of interpolating pre-calculated daylight factors to obtain hourly illuminance and glare reduces computation time by a factor of 200 compared to hourly re-integration over each window.

(3) Hourly lighting control simulation: Stepped and continuously dimming lighting control systems are simulated to determine the electrical lighting energy needed to make up the difference, if any, between the daylighting level and the design illuminance. Finally, the lighting electrical requirements are passed to the thermal calculation which determines hourly heating and cooling requirements for each space and for the building as a whole.

2. DAYLIGHTING PREPROCESSOR

For each daylit space, the preprocessor calculates a set of daylight factors for a series of sun positions covering the annual range of solar altitude and azimuth at the specified building latitude. These factors relate interior illuminance and glare levels to outdoor daylight levels.

2.1 Interior illuminance components

DOE-2 separates daylight incident on a window into two components: (1) sky-related light, i.e., light which originates from the sky, and reaches the window directly or by reflection from exterior surfaces; and (2) sun-related light, i.e., light which originates from the sun, and reaches the window directly or by reflection from exterior surfaces. Light from the window then reaches the workplane directly or via reflection from the interior surfaces of the room.

Figure 1a-e shows schematically the various paths by which diffuse light originating from the sky can pass through a bare, transparent window and reach a reference point on the workplane. Figure 1f-j shows similar paths for light originating from the sun. Figure 2a-f shows the situation in which the window is covered by a diffusing shade.

For a given sun position and sky condition (clear or overcast), the sky-related interior daylight will be proportional to the exterior horizontal illuminance, E_{sky}, due to light from the sky. Similarly, the sun-related interior daylight will be proportional to the exterior horizontal solar illuminance E_s.

2.2 Daylight factors

The following six ratios (daylight factors) are calculated and stored for later use in the hourly calculation of interior daylight illuminance and window glare:

$d_{sky} =$ *(interior illuminance due to sky-related light)* / E_{sky}

$d_s =$ *(interior illuminance due to sun-related light)* / E_s

$w_{sky} =$ *(average window luminance due to sky-related light)* / E_{sky}

$w_s =$ *(average window luminance due to sun-related light)* / E_s

$b_{sky} =$ *(window surround (background) luminance due to sky-related light)* / E_{sky}

$b_s =$ *(window surround (background) luminance due to sun-related light)* / E_s

These factors depend on **room conditions**, such as room geometry, surface reflectances, reference point location, window size and orientation, glass transmittance, and window shade transmittance; and on **exterior conditions**, such as ground reflectance, location and reflectance of external obstructions, condition of sky, and position of sun.

The six daylight factors are calculated for each of the following combinations of reference point, window, sky condition, sun position, and shading device:

$$\begin{bmatrix} \textit{Ref. pt. \#1} \\ \textit{(and \#2} \\ \textit{if defined)} \end{bmatrix} \begin{bmatrix} \textit{Window \#1} \\ \textit{Window \#2} \\ \cdot \\ \cdot \\ \cdot \\ \textit{Window \#}N_w \end{bmatrix} \begin{bmatrix} \textit{Clear sky,} \\ \textit{sun pos. \#1} \\ \cdot \\ \cdot \\ \cdot \\ \textit{Clear sky,} \\ \textit{sun pos. \#20} \\ \textit{Overcast sky} \end{bmatrix} \begin{bmatrix} \textit{Bare window} \\ \textit{Window plus shade} \end{bmatrix}$$

For example, for a room with one reference point, one window, and no window-shade, there are (1 x 1 x 21 x 1) x 6 = 126 daylight factors. In the Northern hemisphere the 20 sun positions for the clear sky case cover a grid of five equally-spaced solar azimuths from 70° to 290° (measured clockwise from North), and four equally-spaced altitudes from 10° (5° for latitudes above 48°) to the maximum altitude reached by the sun at the latitude in question. Figure 3 shows the sun positions for 40° N latitude.

2.3 Calculation of exterior illuminance

The equations used to calculate exterior illuminance are based on empirical formulations for standard clear and overcast skies adopted by the Commission Internationale de l'Eclairage (CIE) [3]. These equations are based on the European work of Kittler [4], Krochmann [5], Dogniaux [6], and others.

2.3.1 Direct Solar Illuminance

The horizontal direct solar illuminance at the earth's surface under clear sky conditions can be expressed as [6,7]

$$E_s = E_{DN}^o \, e^{-\bar{a} m T} \, sin\phi_s \tag{1}$$

where E_{DN}^o is the extraterrestrial direct normal illuminance, ϕ_s is the altitude of the sun, m is the optical air mass, T is the atmospheric turbidity, and $\bar{a}$ is an empirically determined atmospheric extinction coefficient. The turbidity is a measure of the aerosol and moisture content of the atmosphere. It has the form [6,7]

$$T = \left[\frac{\phi_{s,deg} + 85}{39.5 \, e^{-w} + 47.4} + 0.1 \right] + (16 + 0.22w)\,\beta \tag{2}$$

The quantity w is the amount of precipitable water vapor in the atmosphere [cm of water]; w ranges from 0.5-1.0 for desert air, to 5 and above for tropical conditions. The Angstrom turbidity coefficient, β, depends on the amount of aerosols (particulates and water droplets) in the air. Typical values of β range from 0.05 to 0.20. The value of T ranges from about 2 for a very clean, dry atmosphere, to 5 and above for moist, polluted conditions. In DOE-2, monthly average values of w and β are entered from tables of measured values for different locations in the United States [8-10].

Dogniaux [6] gives the following parameterizations for the quantities $\bar{a}$, m and E_{DN}^o in eqn. (1):

$$\begin{aligned} \bar{a} &= 0.1512 - 0.0262T \;\; for \; \beta < 0.075, \\ &= 0.1656 - 0.0215T \;\; for \; 0.075 \leq \beta < 0.15, \\ &= 0.2021 - 0.0193T \;\; for \; \beta \geq 0.15; \end{aligned} \tag{3}$$

$$m = (1-0.1h)/[\sin\phi_s + 0.15(\phi_s + 3.885)^{-1.253}] \,, \tag{4}$$

where h is the building altitude in km; and

$$E^{o}_{DN}\ [klx] = 126.82 + 4.248\cos\omega J + 0.08250\cos 2\omega J$$

$$- 0.00043\cos 3\omega J + 0.1691\sin\omega J \tag{5}$$

$$+ 0.00914\sin 2\omega J + 0.01726\sin\omega J,$$

where J is the number of the day of the year and $\omega = 2\pi/366$. The dependence on J accounts for the variation of the solar constant with changing earth-sun distance.

2.3.2 Diffuse illuminance

The illuminance, E_{sky}, on an unobstructed horizontal plane due to diffuse radiation from the sky is calculated by DOE-2 for clear sky and for overcast sky by integrating over the appropriate sky luminance distribution, L:

$$E_{sky} = \int_0^{2\pi} \int_0^{\pi/2} L\ (\theta_{sky}, \phi_{sky})\ \sin\phi_{sky} \cos\phi_{sky}\ d\,\theta_{sky}\ d\,\phi_{sky} \,, \tag{6}$$

where θ_{sky}, ϕ_{sky} are the azimuth and altitude, respectively, of a sky element and E_{sky} is in klx if L is in kcd/m^2.

Clear sky. For clear skies, the luminance distribution derived by Kittler [4,3] from measurements in Europe is used. It has the form

$$L(\theta_{sky}, \phi_{sky}) = L_z(\phi_s)\ \frac{(0.91+10e^{-3\gamma}+0.45\cos^2\gamma)(1-e^{-0.32\,\mathrm{cosec}\,\phi_{sky}})}{.27385\ (0.91+10e^{-3(\pi/2-\phi_s)}+0.45\sin^2\phi_s)} \tag{7}$$

where ϕ_S is the altitude of sun, L_z is the zenith luminance of the sky, and γ is the opening angle between sun and sky element. A contour plot of the ratio $L(\theta_{sky},\phi_{sky})/L_z$ is shown in Fig. 4 for a solar altitude of 40°. The general characteristics of the distribution are a large peak near the sun; a minimum at a point on the other side of the zenith from the sun; and an increase in luminance as the horizon is approached.

The zenith luminance in eqn. (7) is given by [11]

$$L_z[kcd/m^2] = (1.34T\text{-}3.46)\tan\phi_s + 0.10T + 0.90, \quad \phi_s \leq 60° \text{ and } T>3. \tag{8}$$

For values of T less than 3, this equation is used with T=3.

For $\phi_s > 60°$, where eqn. (8) is invalid, L_z is taken to be

$$L_z(\phi_s) = \frac{3.25 L_z(60^o)\sin\phi_s}{[3.25-.1050(\phi_s-60)+.0010(\phi_s-60)^2]\sin 60^o}, \; \phi_s > 60^o, \tag{9}$$

which was obtained [12] by constraining the horizontal illuminance to increase as $\sin\phi_s$ for $\phi_s >$ 60°.

The clear sky diffuse horizontal illuminance, E_{cl}, is obtained by inserting eqn. (7) into eqn. (6) and evaluating the double integral using Simpson's rule.

Overcast sky. The CIE standard overcast sky luminance distribution has the form [13]

$$L_{oc}(\phi_{sky}) = L_{z,oc}\frac{1+2\sin\phi_{sky}}{3}, \tag{10}$$

where the zenith luminance, $L_{z,oc}$, is [5]

$$L_{z,oc}\,[kcd/m^2] = 0.123 + 8.6\sin\phi_s\,. \tag{11}$$

The overcast sky luminance distribution, unlike the clear sky case, does not depend on either the solar azimuth or the sky azimuth. The zenith is three times brighter than the horizon.

Using the above equation for L_{oc} in eqn. (6) yields the following expression for the exterior horizontal illuminance from an overcast sky:

$$E_{oc}[klx] = \frac{7\pi}{9} L_{z,oc}[kcd/m^2] = 0.3 + 21.1 \sin\phi_s. \qquad (12)$$

This is plotted in Fig. 5.

2.3.3 Luminous efficacy of solar radiation

If measured solar irradiance values are present on the DOE-2 weather file, the luminous efficacy in lumens/watt is calculated for direct solar radiation, clear sky diffuse solar radiation, and overcast sky diffuse solar radiation. These efficacies, multiplied by solar irradiance, are used to obtain hourly exterior illuminance values, as described below in Section 3.1.

Direct solar radiation. The luminous efficacy of direct solar radiation as parameterized by Dogniaux [6,7] is

$$K_s\ [lm/W] = K_o\ e^{-mT(\bar{a}-\bar{a}_s)} \qquad (13)$$

where K_o is the extraterrestrial luminous efficacy (93.73 lm/W) and $\bar{a}_s$, the atmospheric extinction coefficient due to Rayleigh scattering of solar radiation, is given by

$$\bar{a}_s = 1.4899 - 2.1099 \cos\phi_s + 0.6322 \cos2\phi_s + 0.0252 \cos3\phi_s$$

$$- 1.0022 \sin\phi_s + 1.0077 \sin2\phi_s - 0.2606 \sin3\phi_s \qquad (14)$$

K_s is plotted as a function of solar altitude for high and low values of atmospheric moisture, w, and decadic turbidity factor, $B (B = 1.07\beta)$ in Fig. 6. The rapid fall-off in K_s for $\phi_s < 30^\circ$ is primarily due to the λ^{-4} wavelength dependence of Rayleigh scattering. K_s increases with w since the absorption of solar radiation by atmospheric water vapor is much higher in the infrared than the visible.

Diffuse solar radiation. The luminous efficacy, K_{cl}, of clear sky diffuse radiation as a function of B, w, and solar altitude is shown in Fig. 7, which is derived from Table 4 of Aydinli [14]. Aydinli's values are based on calculations [14,15] taking into account the spectral distribution of extraterrestrial solar radiation, Rayleigh scattering, aerosol scattering and absorption by water vapor and ozone. The figure shows that K_{cl} varies from 115 to 135 lm/W, with a mean value of 125.4 lm/W and standard deviation of 6.1 lm/W. Because of the relatively small standard deviation in K_{cl} ($\pm 5\%$), the mean value of K_{cl} is used in DOE-2.

For an overcast sky, the luminous efficacy K_{oc} is assigned a constant value of 110 lm/W [7].

2.4 Calculation of interior illuminance

2.4.1 Direct component

The direct daylight illuminance E_d from a window is determined by dividing the window into an x-y grid and finding the flux reaching the reference point directly (i.e., without interior reflection) from each grid element. The net direct horizontal illuminance from the window is the sum of the contributions from all the window elements which lie above the workplane:

$$E_d = \sum L_w \, d\omega \cos\psi \,, \tag{15}$$

where L_w is the luminance of the window element as seen from the reference point, $d\omega$ is the solid angle subtended by the window element with respect to the reference point, and ψ is the angle between the vertical and the ray from the reference point to center of the window element.

Bare window. For the bare window case, the luminance L_w of the window element is found by projecting the ray which connects reference point and window element and determining whether it intersects the sky or an exterior obstruction. (It is assumed that there are no internal obstructions.) If L is the corresponding luminance of sky or exterior obstruction, the window luminance is $LT_g(\eta)$, where T_g is the visible transmittance of the glass for incidence angle η.

Window with shade. For the window-plus-shade case, the shade is assumed to be a perfect diffuser, i.e., the luminance of the shade, L_{sh}, is independent of angle of emission of light, position on shade, and angle of incidence of exterior light falling on the shade. The illuminance contribution at the reference point from a shade element is given by eqn. (15) with $L_w = L_{sh}$ if the shade is inside the window, or $L_w = L_{sh} T_g(\eta')$ if the shade is outside the window, where η' is the angle of emission of light from the shade.

2.4.2 Internally reflected component

Daylight reaching a reference point after reflection from interior surfaces is calculated using the "split-flux" method [16,17]. The daylight transmitted by the window is split into two parts -- a downward-going flux, Φ_{FW} [lm], which falls on the floor and portions of the walls below the imaginary horizontal plane passing through the center of the window ("window midplane"), and an upward-going flux Φ_{CW} [lm], which strikes the ceiling and portions of the walls above the window midplane (see Fig. 8). A fraction of Φ_{FW} and Φ_{CW} is absorbed by the room surfaces. The remainder, the first-reflected flux, F_1, is approximated by

$$F_1 = \Phi_{FW}\,\rho_{FW} + \Phi_{CW}\,\rho_{CW}\,, \tag{16}$$

where ρ_{FW} is the area-weighted average reflectance of the floor and those parts of the walls below the window mid-plane, and ρ_{CW} is the area-weighted average reflectance of the ceiling and those parts of the walls above the window mid-plane.

A flux balance is used to find the final average internally-reflected illuminance E_r (which in this method is uniform throughout the room). The total reflected flux absorbed by the room surfaces (or lost through the windows) is $AE_r\,(1-\rho)$, where A is the total inside surface area of the floors, walls, ceiling, and windows in the room, and ρ is the area-weighted average reflectance of the room surfaces, including windows. From conservation of energy,

$$F_1 = A\ E_r\ (1-\rho) \tag{17}$$

Substituting this in eqn. (16) gives

$$E_r\ [lm/unit\text{-}area] = \frac{\Phi_{FW}\,\rho_{FW} + \Phi_{CW}\,\rho_{CW}}{A(1-\rho)}\,. \tag{18}$$

This procedure assumes that the room behaves like an integrating sphere with perfectly diffusing interior surfaces and no internal obstructions. It therefore works best for rooms which are close to cubical in shape, have matte surfaces (which is usually the case), and have no internal partitions. For these reasons, the split-flux method is not recommended for rooms whose depth measured from the window-wall is more than approximately three times greater than ceiling height; in this case the method can overpredict the internally-reflected illuminance near the back of the room by a factor of two or more (see Section 5 and Fig. 12c-f).

Transmitted flux from sky and ground. The luminous flux incident on the center of the window from a luminous element of sky, ground, or external obstruction at angular position (θ,ϕ), of luminance $L\ (\theta,\phi)$, and subtending a solid angle $\cos\phi\, d\theta\, d\phi$ is

$$d\Phi_{inc} = A_W\ L(\theta,\phi)\ \cos\eta\ \cos\phi\, d\theta\, d\phi \tag{19}$$

where A_W is the window area, and $d\Phi_{inc}$ is in lm if L is in cd/unit-area. The transmitted flux is

$$d\Phi = d\Phi_{inc}\ T_w$$

where T_w is the window transmittance. If $T_g(\eta)$ is the glass transmittance for incidence angle η, $T_{g,dif}$ is the glass transmittance for diffuse illuminance, and T_{sh} is the shade transmittance, then

$T_w = T_g(\eta)$ for unshaded glass,

$= T_g(\eta) T_{sh}$ for glass with inside shading device,

$= T_{sh} T_{g,dif}$ for glass with outside shading device.

For a bare window of arbitrary tilt the total downgoing transmitted flux, Φ_{FW}, is obtained by integrating $d\Phi$ over the part of the exterior hemisphere seen by the window which lies above the window midplane. This gives

$$\Phi_{FW,bare} = A_w \int_0^{\pi/2} d\phi \int_{-\theta_{max}}^{\theta_{max}} L(\theta,\phi)\ \cos\eta\, T_g(\eta)\ \cos\phi\, d\theta \tag{20}$$

where, if ϕ_w is the altitude angle of the outward normal to the window,

$\theta_{max} = |\cos^{-1}(-\tan\phi \tan\phi_w)|$ (see ref. 12).

The upgoing flux, $\Phi_{CW,bare}$, is similarly obtained by integrating over the part of the exterior hemisphere which lies below the window midplane:

$$\Phi_{CW,bare} = A_w \int_{\pi/2-\phi_w}^{0} d\phi \int_{-\theta_{max}}^{\theta_{max}} L(\theta,\phi) \cos\eta \, T_g(\eta) \cos\phi \, d\theta \tag{21}$$

For a window with a diffusing shade, the total transmitted flux is first calculated:

$$\Phi = A_w \int_{\pi/2-\phi_w}^{\pi/2} d\phi \int_{-\theta_{max}}^{\theta_{max}} L(\theta,\phi) \cos\eta \, T_w(\eta) \cos\phi \, d\theta \tag{22}$$

This is then divided into up- and down-going portions given, respectively, by

$$\Phi_{FW,sh} = \Phi(1-f) \text{ and } \Phi_{CW,sh} = \Phi f \ , \tag{23}$$

where f is the fraction of the hemisphere seen by the inside of the window which lies above the window midplane. For a vertical window, f=0.5, and the up- and down-going transmitted fluxes are equal: $\Phi_{FW,sh}=\Phi_{CW,sh}=\Phi/2$. For a horizontal skylight, f=0, giving $\Phi_{FW,sh}=\Phi$ and $\Phi_{CW,sh}=0$.

Flux from sun. The incident luminous flux from direct sun striking the window at incidence angle η is

$$\Phi_{inc} = A_w \, E_{DN} \cos\eta \, (1-f_{shaded}) \ , \ \cos\eta \geq 0 \tag{24}$$

$$= 0 \ , \ \cos\eta < 0 \ ,$$

where E_{DN} is the direct normal solar illuminance and f_{shaded} is the fraction of window which is shaded by obstructions such as fins, overhangs, or neighboring buildings.

The transmitted flux is $\Phi=T_w(\eta)\Phi_{inc}$. For a bare window, $\Phi_{FW,bare}=\Phi$ and $\Phi_{CW,bare}=0$, i.e., all of the transmitted flux is downward since the sun always lies above the window midplane. For a window with a diffusing shade, $\Phi_{FW,sh}=\Phi(1-f)$ and $\Phi_{CW,sh}=\Phi f$.

Window shade luminance. The window shade luminance is determined at the same time that the transmitted flux is calculated. It is given by

$$L_{sh} = \frac{1}{\pi} \int_{\frac{\pi}{2}-\phi_w}^{\pi/2} d\phi \int_{\theta_{min}}^{\theta_{max}} L(\theta,\phi)\cos\eta\, T_m \cos\phi\, d\theta \tag{25}$$

where T_m is equal to T_{sh} for an outside shade and is equal to $T_g\ (\eta)\ T_{sh}$ for an inside shade.

2.5 Calculation of discomfort glare from windows

Since discomfort glare is subjective, it is difficult to quantify and the reliability of existing parameterizations is controversial [18]. For DOE-2, we have chosen the formulation of Hopkinson [19,20] as being the best available at the present time. In this formulation the discomfort glare at a reference point due to luminance contrast between a window and the interior surfaces surrounding the window is given by

$$G = \frac{0.48\, L_w^{1.6}\ \Omega^{0.8}}{L_b + 0.07\ \omega^{0.5}\ L_w} \tag{26}$$

where G is the discomfort glare constant, L_w is the average luminance of the window as seen from the reference point (cd/m^2), ω is the solid angle subtended by the window with respect to reference point, Ω is the solid angle subtended by the window and modified to take direction of occupant view into account, and L_b is the average luminance of the background area surrounding the window (cd/m^2).

Dividing the window into N_x by N_y rectangular elements, as is done for calculating the direct component of interior illuminance, gives

$$L_w = \frac{1}{N_x N_y} \sum_{j=1}^{N_y} \sum_{i=1}^{N_x} L_w(i,j) \qquad (27)$$

where $L_w\ (i,j)$ is the luminance of element (i,j) as seen from the reference point. Similarly,

$$\omega = \sum_{j=1}^{N_y} \sum_{i=1}^{N_x} d\omega\,(i,j) \qquad (28)$$

where $d\omega(i,j)$ is the solid angle subtended by the $(i,j)^{th}$ element with respect to the reference point. The modified solid angle, Ω, is

$$\Omega = \sum_{j=1}^{N_y} \sum_{i=1}^{N_x} d\omega\,(i,j)\, p(i,j) \qquad (29)$$

where $p(i,j)$ is an empirically determined "position factor" [21,12] which accounts for the rapid decrease in visual excitation as the displacement angle between the luminous window element and the line of sight increases. Values of p at selected values of horizontal and vertical displacement angle are shown in Table 1. Intermediate values are obtained by interpolation. The direction of the line of sight is a user-defined input parameter.

The background luminance is given by $L_b = E_b \rho_b$, where E_b is the average illuminance on the floor, wall, and ceiling surfaces surrounding the window; ρ_b is the average reflectance of these surfaces. In DOE-2, ρ_b is approximated by the average interior surface reflectance, ρ, of the entire room. E_b is approximated by the larger of E_r and E_{set}, where E_r is the total internally-reflected component of daylight illuminance produced by all the windows in the room; E_{set} is the illuminance setpoint at the reference point at which glare is being calculated. A precise calculation of L_b is not required since the glare index (described below) is logarithmic: a factor of two variation in L_b generally produces a change of less than 1.0 in the glare index.

The net daylight glare at a reference point due to all of the windows in a room is expressed in terms of a glare index, GI, which is given by

$$GI = 10\log_{10} \sum_{i=1}^{N_W} G_i \tag{30}$$

where G_i is the glare constant at the reference point due to the i^{th} window. The recommended maximum allowable values of GI depend on space function. Typical values are 18 for hospital wards, 20 for school classrooms and drafting, and 22 for general office work [22].

The glare formulation used in DOE-2 does not account for glare caused by penetration of beam radiation into a room through unshaded windows. However, admittance of direct solar gain in spaces requiring good visual performance is usually not good design practice. Therefore, windows lacking fixed architectural elements such as fins or overhangs to block direct sun would normally have operable shading systems (e.g. shades, blinds, draperies) to control direct sun when it is present. Deployment of these devices can be simulated using the window management option with a user-defined direct solar gain setpoint. The program then calculates the transmitted radiation through the unshaded window each hour and deploys the shading device whenever the transmitted radiation exceeds the trigger level.

3. HOURLY DAYLIGHTING CALCULATION

A daylighting calculation is performed each hour that the sun is up. The exterior horizontal illuminance from sun and sky is calculated theoretically for the current-hour sun position and cloud amount, or is determined from solar irradiance data if present on the weather file. The interior illuminance at each reference point is found for each window by interpolating the illuminance factors calculated by the preprocessor. By summation, the net illuminance and glare due to all the windows in a space are found. If glare or solar gain exceed user-specified thresholds, window shading devices can be deployed. The daylight illuminance at each reference point for the final window-shade configuration is used by the lighting control system simulation to determine the electric lighting power required to meet the illuminance setpoint.

3.1 Hourly exterior daylight availability

For the current-hour sun position and current-month atmospheric moisture and turbidity, eqns. (10) and (13) are used to obtain the exterior horizontal illuminance from a standard clear sky (E_{cl}) and from a standard overcast sky (E_{oc}). If the weather file has solar irradiance data, the program finds the current-hour luminous efficacy, K_s, for standard clear sky direct solar radiation using eqn. (14).

Because few data exist on the luminous characteristics of partly-cloudy skies, we have assumed that, to first approximation, the sky in a given hour can be divided into a uniformly distributed fraction, η_{cl}, which has the clear sky luminance distribution for the current sun position, and a fraction $\eta_{oc} = 1 - \eta_{cl}$ which has the overcast sky luminance distribution. η_{cl} is taken to be a function of CR, the fraction of the skydome covered with clouds (obtained from the weather file). The form chosen for η_{cl} vs CR, shown in Fig. 9, gives a clear sky luminance distribution for the whole sky for $CR \le 0.2$, which assumes that for low cloud amounts reflection of sunlight from the clouds will, on the average, give a cloud luminance which is comparable to that of the sky. As CR increases above 0.2, the average cloud luminance is assumed to become progressively closer to the standard overcast sky luminance.

The average exterior horizontal illuminance due to the fraction of sky with standard clear sky characteristics is then $\eta_{cl} E_{cl}$. Correspondingly, $\eta_{oc} E_{oc}$ is the exterior horizontal illuminance due to the fraction of sky with standard overcast sky characteristics.

The average direct solar exterior horizontal illuminance for the current hour is taken to be

$$\overline{E_s} = (1 - CR)\, E_s \;, \tag{31}$$

where E_s, the clear-sky solar illuminance, is obtained from eqn. (1).

If the weather file has measured solar radiation data, this expression is replaced by

$$\overline{E_s} = K_s\, I_{DN}^{meas} \sin\phi_s \;, \tag{32}$$

where K_s is the luminous efficacy [lm/W] of solar radiation from eqn. (14), and I_{DN}^{meas} is the measured direct normal solar irradiance [W/m^2]. In addition, the horizontal illuminance values from the clear and overcast portions of the sky are each adjusted by a multiplicative factor α so that their sum equals the measured horizontal diffuse irradiance, I_d^{meas}, times the luminous efficacy. The quantity α is thus obtained from

$$\alpha\,(\eta_{cl}E_{cl} + \eta_{oc}E_{oc}) = I_d^{meas}\,(\eta_{cl}K_{cl} + \eta_{oc}K_{oc}) \tag{33}$$

3.2 Hourly workplane illuminance and window background luminance

The hourly average workplane illuminance at a reference point is given by

$$E = \sum_{i=1}^{N_w} \left[d_s(i,i_{sh})E_s + d_{cl}(i,i_{sh})\eta_{cl}E_{cl} + d_{oc}(i,i_{sh})\eta_{oc}\,E_{oc} \right] \tag{34}$$

where i is the window index; i_{sh} is 1 for open shade and 2 for closed shade; and d_s, d_{cl}, d_{oc}, are daylight factors for sun-related, clear-sky-related, and overcast-sky-related illuminance, respectively. The values of d_s and d_{cl} depend on the current-hour sun position. They are obtained by linearly interpolating, in solar altitude and azimuth, the corresponding daylight factors calculated by the preprocessor.

The current-hour luminance of the area surrounding a window is, similarly,

$$L_b = b_s(i,i_{sh})E_s + b_{cl}(i,i_{sh})\eta_{cl}E_{cl} + b_{oc}(i,i_{sh})\eta_{oc}E_{oc}\ , \tag{35}$$

where b_s, b_{cl}, and b_{oc} are the interpolated daylight factors for background luminance.

The current-hour average luminance of a window is

$$L_{w,i} = w_s(i,i_{sh})E_s + w_{cl}(i,i_{sh})\eta_{cl}E_{cl} + w_{oc}(i,i_{sh})\eta_{oc}E_{oc} \tag{36}$$

where w_s, w_{cl}, and w_{oc} are the interpolated daylight factors for window luminance.

3.3 Hourly glare index

From eqns. (26) and (30), the current-hour glare index at a reference point is

$$GI = 10log_{10} \sum_{i=1}^{N_w} \frac{0.48\, L_{w,i}^{1.6}\, \Omega_i^{0.8}}{L_b' + 0.07\, \omega_i^{0.5}\, L_{w,i}}, \tag{37}$$

where L_b' is the larger of the window surround luminance, L_b, from daylight, and the average surround luminance which would be produced by the electric lighting at full power if the illuminance on the room surfaces were equal to the setpoint illuminance.

3.4 Glare control simulation

If the glare index at either reference point exceeds a user-specified threshold value, GI_{max} shading devices are closed sequentially until the glare index at both points is below GI_{max}. Each time a shading device is closed, the glare index and illuminance at each reference point are recalculated.

3.5 Electric lighting control system simulation

In DOE-2, the user can divide a room into one or two lighting zones. The electric lighting power in each zone is assumed to be controlled by a sensor which responds to the illuminance at the user-specified reference point for that zone. If the daylight illuminance at a reference point is E, the fractional electric light output required to meet a design illuminance value, E_{set}, is

$$f_L = (E_{set} - E) \,/\, E_{set}\,,\ E < E_{set} \tag{38}$$

$$= 0,\ E \geq E_{set}$$

For a continuously dimmable control system, the lighting power curve is assumed to have the linear form in Fig. 10a, which gives fractional electrical input power, f_p, vs. f_L. The quantities $f_{p,min}$ and $f_{L,min}$ in Fig. 10a are user-specified. For a stepped control system, f_p takes on discrete values depending on the range of f_L and the number of steps, as shown in Fig. 10b.

4. DAYLIGHTING OUTPUT REPORTS

The value of energy simulation studies can be limited or enhanced by the quality and quantity of output data available to the program user. In order to determine the real value of daylighting as an energy conservation strategy, it is essential to understand not only the energy savings, but also the time-varying patterns of daylight utilization within each space. We have provided a series of new reports that provide different levels of information on daylighting performance. Careful analysis and interpretation of these reports can speed the process of arriving at a building design that meets required performance criteria. Figure 11 shows four sample daylighting reports for a south-facing office module using a weather file (with measured solar radiaton data) for Madison, Wisconsin. The module is 6.1m wide, 9.2m deep, and is 3.0m floor-to-ceiling. It has a 1.5m high strip window with 0.9m sill height and 90% transmittance. Drapes with 35% transmittance are assumed to be closed by occupants if direct solar transmission exceeds 63 w/m^2 (20 Btu/ft^2-hr) or if glare is excessive ($GI > 22$). There are two independently-controlled lighting zones (each 4.6m deep) with reference points 3.0m and 7.6m respectively from the window-wall, and with design illuminance of 538 lx (50 fc). Each lighting zone has a continuously dimmable control system, as shown in Fig. 10a, with $f_{L,min} = 0.2$ and $f_{p,min} = 0.3$.

Figure 11a provides the type of monthly and annual summary data useful in estimating the savings and cost-effectiveness of a daylighting strategy. The energy savings by hour of day given in Fig. 11b provide details of the hourly/monthly pattern of daylight savings. These results can be observed zone by zone and for the entire building. Figure 11c provides statistics on the frequency of occurrence of various interior daylight illuminance values and on the cumulative probability of exceeding each value. Without rerunning the DOE-2 program, the user can estimate the change in daylighting savings if a design illuminance value is changed or the lighting control strategy is altered.

Figure 11d shows an example of a report with hourly values of daylighting-related variables for a particular day. The quantities appearing in this type of report are selected by the user from a list of about 200 different thermal and daylighting variables. The user also selects the time periods the report is printed, allowing, for example, hourly daylighting profiles to be made for typical days at different times of the year.

In addition to these daylighting-specific reports, DOE-2 produces a variety of reports (not shown) which allow the net energy savings and cost implications of daylighting strategies to be assessed on an hour-by-hour, monthly, or annual basis. These reports are described in ref. [1] and illustrated in sample applications in ref. [23].

5. VALIDATION

Two types of validation studies have been undertaken: (1) Parametric analyses have been done to test the sensitivity of each calculation process to key design parameters. For example, the influence of window size, window transmittance, and interior surface reflectance has been examined under a variety of sun and sky conditions. (2) A three-way comparison has been made among DOE-2, SUPERLITE (a detailed illuminance calculation program [24]), and illuminance measurements made in scale models in the Lawrence Berkeley Laboratory (LBL) sky simulator [25]. Representative results for clear and overcast conditions for a small, single-occupant office model and a deep open-landscape office model are shown in Fig. 12. The difference in the ratio of the three methods is generally $\leq 15\%$ except very near the window (where the illuminance is not of particular interest) and far from the window-wall in the deep model (Fig. 12c-f) where the split-flux method used in DOE-2 overpredicts the inter-reflected illuminance.

Comparisons of DOE-2 with measured energy use in non-daylit buildings has shown [25] that the program can be expected to predict annual energy use to about $\pm 15\%$ if the building's physical characteristics, operating schedules, and HVAC equipment efficiencies are known. Validation of DOE-2 against the measured energy performance of daylit buildings has not yet been carried out.

6. APPLICATIONS

DOE-2, with its integrated daylighting model, has already proved to be a powerful tool for researchers and designers investigating the relationships between fenestration, building energy consumption, and peak electrical demand. For example, DOE-2 has been used for extensive parametric studies to investigate building envelope performance as part of a large effort sponsored by the U.S. Department of Energy to upgrade building energy standards [27]. The program is being used by utilities and other agencies for the formulation of energy conservation policies (see, for example, ref. [28] and [29]). It is also the basic tool for a series of ongoing investigations of the thermal and daylighting impacts of windows and skylights in office buildings [30, 31, 32].

7. FUNCTIONAL VALUE INPUT

A new feature introduced in the DOE-2.1C version of the program allows users to modify the daylighting and thermal loads calculation algorithms by entering FORTRAN-like functions in the program input. This "functional input" capability permits analysis of innovative design alternatives which previously would have required alteration and recompilation of DOE-2 subroutines. Some daylighting-related applications of functional input are as follows:

(1) The user can input daylight factors obtained from scale model photometric measurements. The program would then use these factors instead of the internally calculated values to determine hourly illuminance. This allows DOE-2 to be used for energy analysis of unusually complex daylighting situations.

(2) Advanced glazing materials can be modeled. Examples are angle-selective glazing (with transmittance vs. angle of incidence radically different from the default transmission curves in DOE-2) and glazing whose transmittance is actively or passively controlled by environmental conditions such as glass temperature or incident solar radiation intensity [33].

(3) Complex lighting control schemes can be simulated, including non-linear dimming systems.

(4) The algorithms used to calculate exterior daylight availability can be modified to conform to latest research results on luminous efficacy, partly-cloudy sky luminance distributions, etc.

8. FUTURE DIRECTIONS

The present version of the program (DOE-2.1C) calculates interior illuminance for conventional window designs and simple room geometries using a preprocessor calculation and sun control systems such as shades, drapes, and blinds that are assumed to be ideal diffusers. The program is being expanded to model (1) geometrically complex sunshading solutions, such as louvers and light shelves; (2) designs where internally reflected light is important, such as those with skylights having deep light wells; and (3) unique architectural spaces, such as large atria which provide daylight to adjacent rooms.

Because direct calculation of interior illuminance from complex sunshading systems is difficult and sometimes impossible, a new coefficient-of-utilization (CU) model is being developed which is based on data calculated or measured outside the DOE-2 program. This model includes five coefficients that are sensitive to illumination at the window plane from the ground, sky, and sun. It will be implemented in several ways, as shown schematically by the left-hand branch of fig. 13. Some designs, such as flat-louver systems, can be standardized but may be too complex to calculate in DOE-2. The coefficients for these systems would be precalculated by SUPERLITE (using measured angle-dependent luminance data for the shading devices) and stored in a DOE-2 library. To obtain values for specific products rather than for generic designs, SUPERLITE could be used as a preprocessor to DOE-2, generating the specific coefficients directly.

A second category includes daylighting systems, such as curved semi-specular light shelves, that can be standardized but may be too complex to calculate using existing computational models. In this instance, the required illuminance data would be generated from scale models in the LBL sky simulator under a full range of overcast, clear-sky, and direct-sun conditions. Results would be converted to coefficients and stored in the DOE-2 library.

A third category includes unique designs which will not be found in the DOE-2 library. In this case, a user could develop the required data from model studies, convert these data into a format compatible with the CU calculation, and input the results into the program library. Each user could thus create a personal library of custom designs for evaluation.

A parallel effort is underway to expand the capability of DOE-2 to simulate conduction and solar heat gain through windows with shading devices. This is illustrated by the right-hand branch of fig. 13. Coordinated libraries of solar heat gain coefficients (SHGC's) and CU's will allow the program to accurately simulate the hour-by-hour thermal behavior of complex designs at the same time as interior daylight illuminance is calculated.

Finally, the algorithms used for daylight availability, particularly for overcast and partly-cloudy conditions, and for discomfort glare will be upgraded as new data in these areas become available.

We are thus working towards an energy model that has a high degree of flexibility and should be responsive to the latest in architectural design strategies.

ACKNOWLEDGMENTS

Valuable discussions and information were provided by Eliyahu Ne'eman, LBL/Technion, Robert Clear, LBL (daylight availability), Francis Rubinstein, LBL (lighting controls), Gary Gillette, NBS/National Fenestration Council (daylight availability), W. Frederick Buhl and James J. Hirsch, LBL (DOE-2 structure). The program was tested by Bruce Birdsall (LBL), Steven Gates (California Energy Commission), Paul Hirsch (Argonne National Laboratory), and Richard Johnson (LBL). Mojitaba Navvab and J. J. Kim (LBL) helped in the validation of the program. Editing and word processing were accomplished by Karen H. Olson and Kathleen Ellington.

REFERENCES

1. DOE-2 Reference Manual (Version 2.1A), Los Alamos National Laboratory Report LA-7689-M, Lawrence Berkeley Laboratory Report LBL-8706, 1981, and DOE-2 Supplement (Version 2.1C), Lawrence Berkeley Laboratory Report LBL-8706, Rev. 4, Suppl., 1984.

2. DOE-2 Engineers Manual, Los Alamos National Laboratory Report LA-8520-M, Lawrence Berkeley Laboratory Report LBL-11353, 1982.

3. CIE Technical Committee 4.2, "The Availability of Daylight", Technical Report No. NR, Commission Internationale de l'Eclairage, Paris, 1975.

4. R. Kittler, "Standardization of Outdoor Conditions for the Calculation of the Daylight Factor with Clear Skies", Proc. CIE Inter-Sessional Meeting on Sunlight, Newcastle-Upon-Tyne, 1965.

5. J. Krochmann, "Über die Horizontal Beleuchtungsstärke der Tagesbeleuchtung", Lichttechnik, *15*, 559, 1963.

6. R. Dogniaux, "Représentations Analytiques des Composantes du Rayonnement Lumineux Solaire", L' Institut Royal Météorologique de Belgique - Series A, No. 83.

7. R. Dogniaux and M. Lemoine, "Program for Calculating Solar Irradiance and Illuminance on Oriented and Sloped Surfaces", L'Institut Royal Météorologique de Belgique, 1976

8. George A. Lott, "Precipitable Water Over the United States, Volume 1: Monthly Means", National Oceanic and Atmospheric Administration Technical Report NWS 20, 1976.

9. E. C. Flowers, R. A. McCormick, and K. R. Kurfis, "Atmospheric Turbidity Over the United States, 1961-66", Journal of Applied Meteorology, *8*, 955, 1969.

10. "Global Monitoring of the Environment for Selected Atmospheric Constituents 1977", Environmental Data and Information Service, National Climatic Center, Asheville, NC, 1980.

11. C. Liebelt, "Leuchtdichte- und Strahldichtverteilung des Himmels", Dissertation, Karlsruhe University, 1978.

12. F. C. Winkelmann, "Daylighting Calculation in DOE-2", Report LBL-11353, Lawrence Berkeley Laboratory, Berkeley, CA, 1983.

13. P. Moon and D. E. Spencer, "Illumination from a Non-Uniform Sky", Illum. Engineering, *37*, 707, 1942.

14. S. Aydinli, "The Availability of Solar Radiation and Daylight", Institut für Lichttechnik der Technischen Universität Berlin, 1981.

15. S. Aydinli, "Über die Berechnung der zur Verfügung Stehenden Solar Energie und des Tageslichtes", Verein Deutscher Ingenieure, VDI-Verlage GmbH Dusseldorf, Reiche 6, Nr. 79, 1981.

16. R. G. Hopkinson, J. Longmore, and P. Petherbridge, "An Empirical Formula for the Computation of the Indirect Component of Daylight Factors", Trans. Illum. Eng. Soc. (London), *19*, 201, 1954.

17. J. A. Lynes, "Principles of Natural Lighting", Applied Science Publishers, Ltd., London, 1968, P. 129.

18. H. D. Einhorn, "Discomfort Glare: a Formula to Bridge Differences", Lighting Research and Technology, *11*, 90, 1979.

19. R. G. Hopkinson, "Glare from Windows", Construction Research and Development Journal, *2*, 98, 1970.

20. R. G. Hopkinson, "Glare from Daylighting in Buildings", Applied Ergonomics, *3*, 206, 1972.

21. P. Petherbridge, and J. Longmore, "Solid Angles Applied to Visual Comfort Problems", Light and Lighting, *47*, 173, 1954.

22. R. G. Hopkinson, P. Petherbridge, and J. Longmore, "Daylighting", Heinneman, London, P. 322, 1966.

23. Building Energy Simulation Group, "DOE-2 Sample Run Book, Version 2.1C", Lawrence Berkeley Laboratory Report LBL-8678, 1984.

24. M. F. Modest, "A General Model for the Calculation of Daylighting in Interior Spaces", Energy and Buildings, *5*, 69, 1982.

25. S. Selkowitz, "A Hemispherical Sky Simulator for Daylighting Model Studies", Proceedings of the Sixth National Passive Solar Conference, Portland, Oregon, 1981.

26. S. C. Diamond, B. D. Hunn, C. C. Capiello, "DOE-2 Verification Project Phase I Interim Report", report LA-8295-MS, Los Alamos National Laboratory, 1981.

27. R. Johnson, R. Sullivan, S. Nozaki, S. Selkowitz, C. Conner, and D. Arasteh, "Building Envelope Thermal and Daylighting Analysis in Support of Recommendations to Upgrade ASHRAE/IES Standard 90 – Final Report", Report LBL-16770, Lawrence Berkeley Laboratory, Berkeley, CA, 1983.

28. S. Gates and J. Wilcox, "Daylighting Analysis for classrooms Using DOE-2.1B", Energy and Buildings 6, 331, 1984.

29. G. D. Ander and E. A. Hassan, "System Impacts of Fenestration", Proc. of the Daylighting Applications Conference, American Solar Energy Society, Boulder, CO, 1985.

30. R. Johnson, R. Sullivan, S. Selkowitz, S. Nozaki, C. Conner, and D. Arasteh, "Glazing Energy Performance and Design Optimization with Daylighting", Energy and Buildings *6*, 305, 1984

31. "The Impact of Daylighting on Peak Electrical Demand", U. S. Choi, R. Johnson, and S. Selkowitz, Energy and Buildings *6*, 387, 1984

32. "Energy Performance and Savings Potentials with Skylights", D. Arasteh, R. Johnson, S. Selkowitz, and R. Sullivan, Lawrence Berkeley Laboratory Report LBL-17457, Berkeley, CA, 1984.

33. "Advanced Optical Materials for Daylighting In Office Buildings", Lawrence Berkeley Laboratory Report LBL-20080, Berkeley, CA, 1985.

FIGURE CAPTIONS

Fig. 1. Paths by which light originating from sky (a-e) and from sun (f-j) can reach workplane through a transparent window without a shading device.

Fig. 2. Paths by which light originating from sky (a-c) and from sun (d-f) can reach workplane through a transparent window with a diffusing shading device.

Fig. 3. Sun positions (•) used by preprocessor for calculation of clear sky daylight factors for 40° north latitude. (Sunchart reproduced from "The Passive Solar Energy Book", Edward Mazria, Rodale Press, Emmaus, PA 1979.)

Fig. 4. Clear sky luminance distribution (normalized to unit zenith luminance) for a solar altitude of 40° [Ref 9.].

Fig. 5. Exterior horizontal illuminance from standard overcast sky vs. solar altitude.

Fig. 6. Luminous efficacy of direct solar radiation for selected values of atmospheric moisture, w, and decadic turbidity coefficient,

B (B $\simeq$ 1.07 β).

Fig. 7. Luminous efficacy of clear sky diffuse solar radiation as a function of solar altitude, decadic turbidity factor, B (B $\simeq$ 1.07 β), and atmospheric moisture, w. Based on Aydinli [Ref. 14].

Fig. 8. Vertical section showing up- and down-going transmitted fluxes, ϕ_{CW} and ϕ_{FW}, used in split-flux calculation of the internally-reflected component of interior illuminance.

Fig. 9. Effective fraction of sky, η_{cl}, having standard clear sky luminous distribution vs fraction of sky covered by clouds. The remainder of the sky, 1-η_{cl}, is assumed to have a standard overcast sky luminance distribution.

Fig. 10. Lighting control curves for (a) continuously dimmable system, and (b) stepped system.

Fig. 11. Sample DOE-2 daylighting program reports for the south-facing office module described in text. Selected months only are shown in (a)-(c). Quantities under "REPORT SCHEDULE HOURS" in (a) are restricted to a user-selected time period 8:00am to 5:00pm, the hours of major occupancy. The hourly report in (d) is for sun-up hours on April 2; in this example "CLOUD AMOUNT" is the fraction of sky covered by clouds, in tenths; "EXT ILL CLR SKY" and "EXT ILL OVR SKY" are the exterior horizontal illuminance from the clear and overcast portions of the sky, respectively; "SHADING FLAG" is 1 if window drapes are open, 2 if closed; "LTPW MUL" is the multiplier on electric lighting power due to dimming of lights.

Fig. 12. (a)-(f): SUPERLITE (o) and DOE-2 (■) predictions compared with sky-simulator measurements (-) made along centerline of different scale models. Cases of clear sky have solar altitude 50°, azimuth 0°, but exclude direct sun. Ground reflectance is zero. Interior reflectances are 25% for floor, 60% for walls, 80% for ceiling. Glass transmittance is 90%; diffuser transmittance in (e) is 60%.

Fig. 13. Schematic showing key elements of algorithm development in progress to improve the fenestration modeling capabilities of DOE-2.

TABLE 1

Position Factor, p, for the Glare Calculation

		Horizontal Displacement Angle						
		0°	26°	45°	56°	63°	72°	>72°
	0°	1.0	.492	.226	.128	.081	.057	.0
Vertical	26°	.123	.119	.065	.043	.029	.023	.0
Displacement	45°	.019	.026	.019	.016	.014	.011	.0
Angle	56°	.008	.008	.008	.008	.008	.006	.0
	63°	.0	.0	.003	.003	.003	.003	.0
	>63°	.0	.0	.0	.0	.0	.0	.0

Bare window

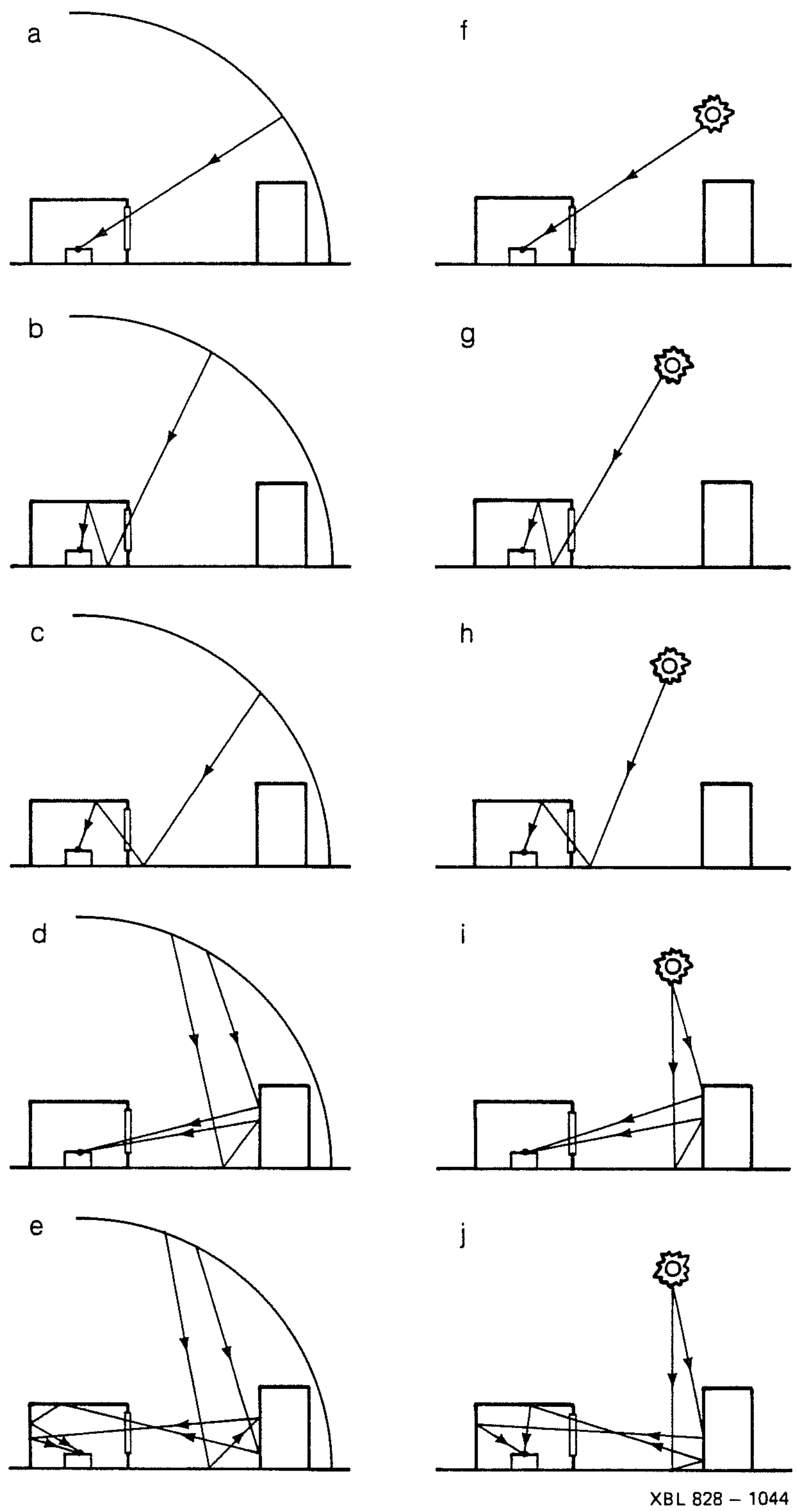

Fig. 1

Window with diffusing shade

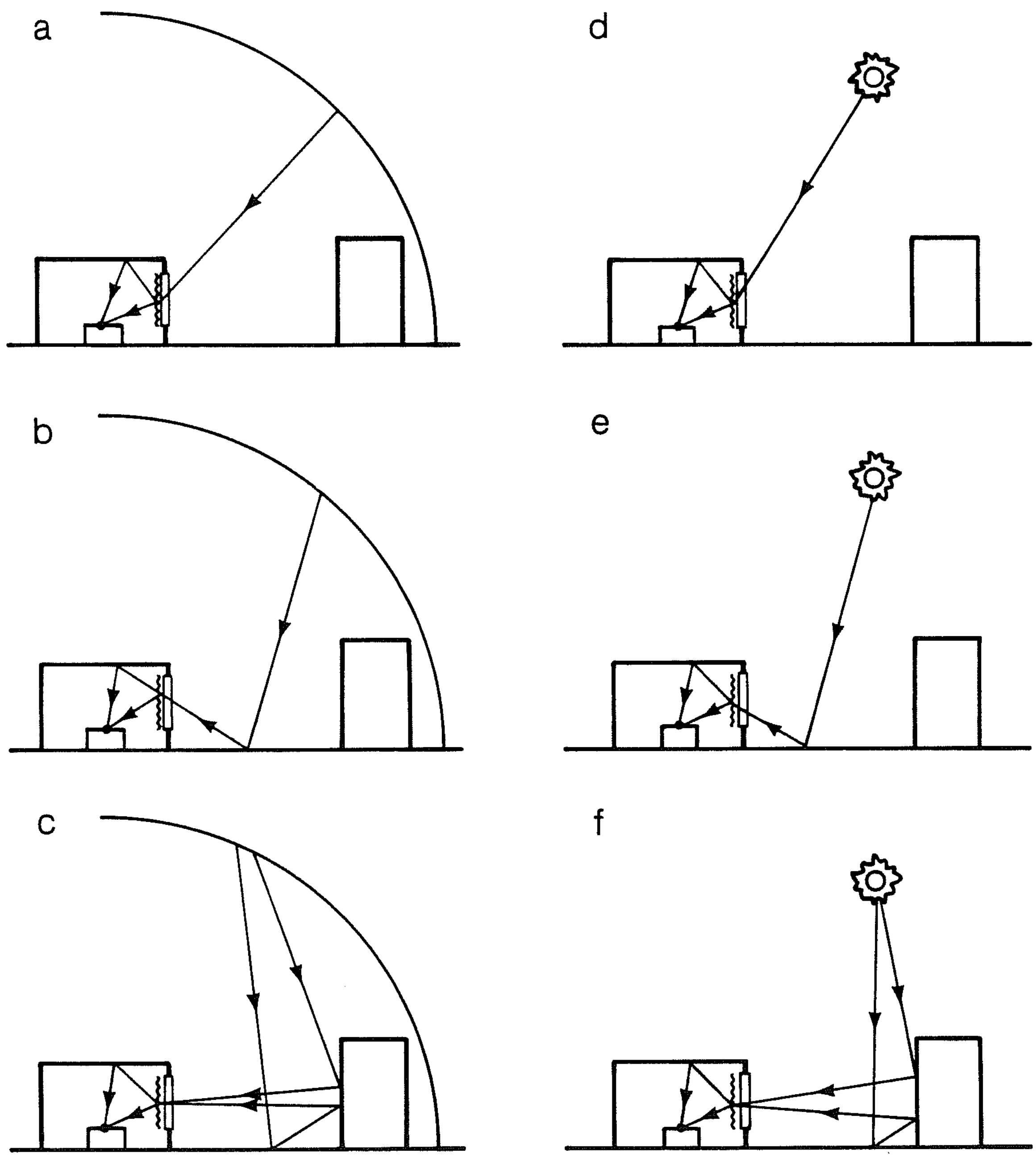

XBL 828-1045

Fig. 2

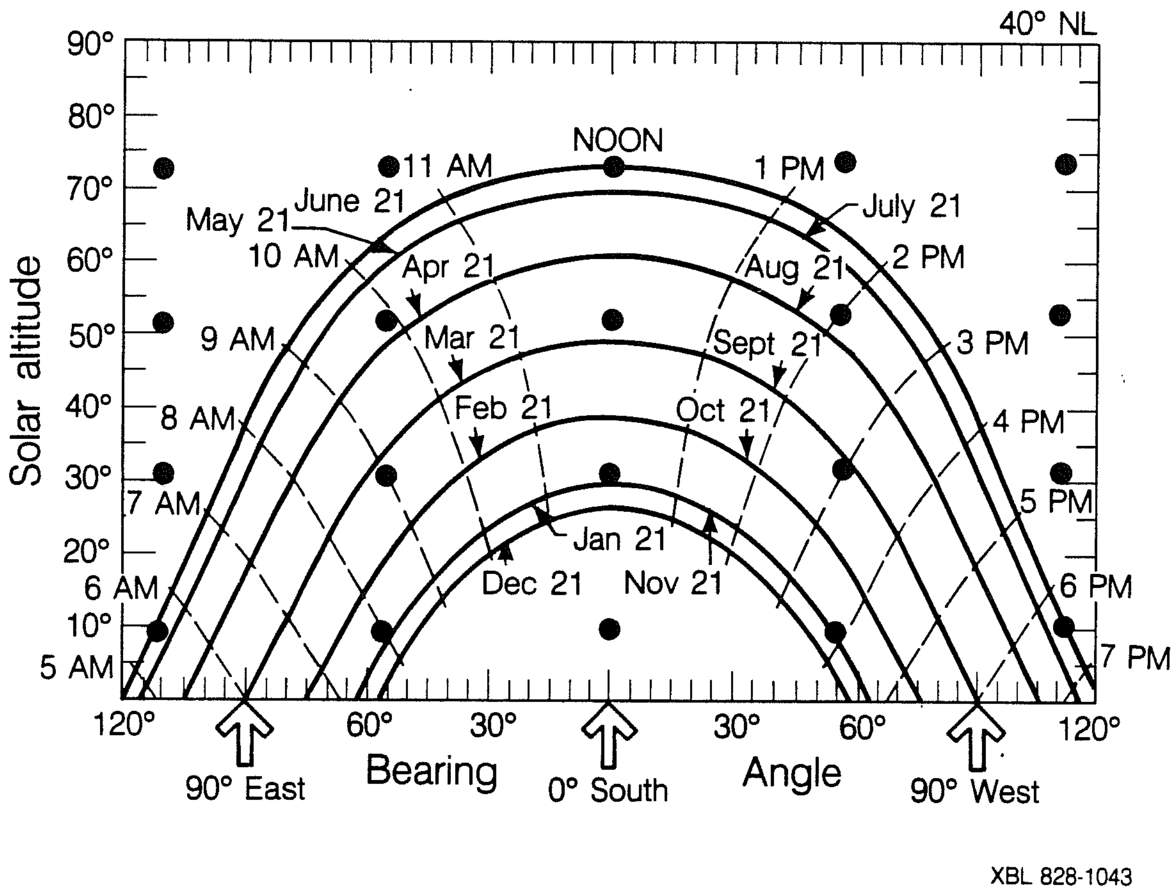
40° NL
90°
80°
70°
60°
50°
40°
30°
20°
10°
Solar altitude
NOON
11 AM
1 PM
June 21
May 21
July 21
10 AM
Apr 21
Aug 21
2 PM
9 AM
Mar 21
Sept 21
3 PM
8 AM
Feb 21
Oct 21
4 PM
7 AM
5 PM
Jan 21
Dec 21
Nov 21
6 AM
6 PM
5 AM
7 PM
120°
60°
30°
30°
60°
120°
90° East
Bearing
0° South
Angle
90° West
XBL 828-1043

Fig. 3

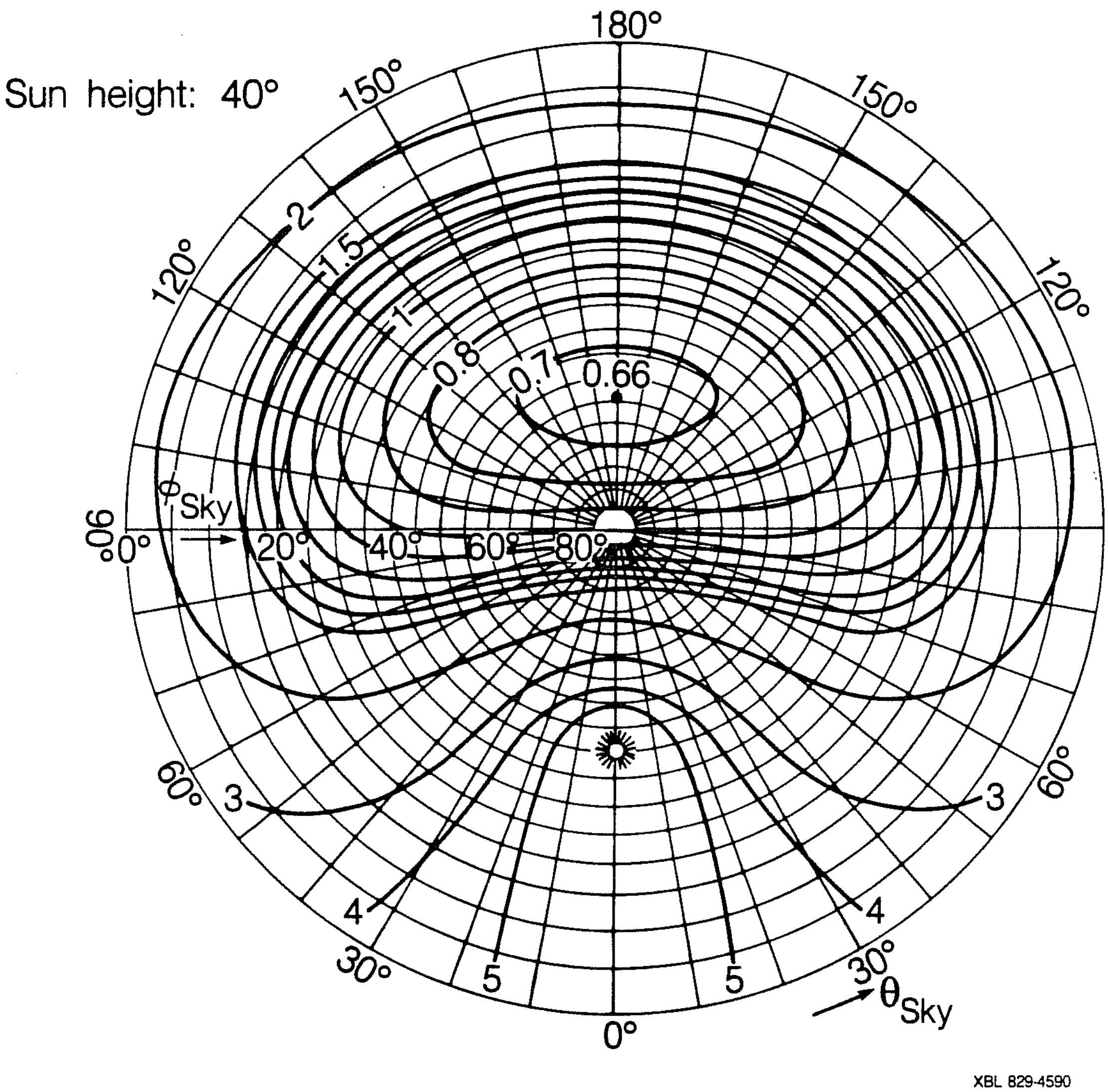

Sun height: 40°
180°
150°
150°
120°
120°
90°
90°
60°
60°
30°
30°
0°
2
1.5
1
0.8
0.7
0.66
φ Sky
0°
20°
40°
60°
80°
3
3
4
4
5
5
θ Sky
XBL 829-4590

Fig. 4

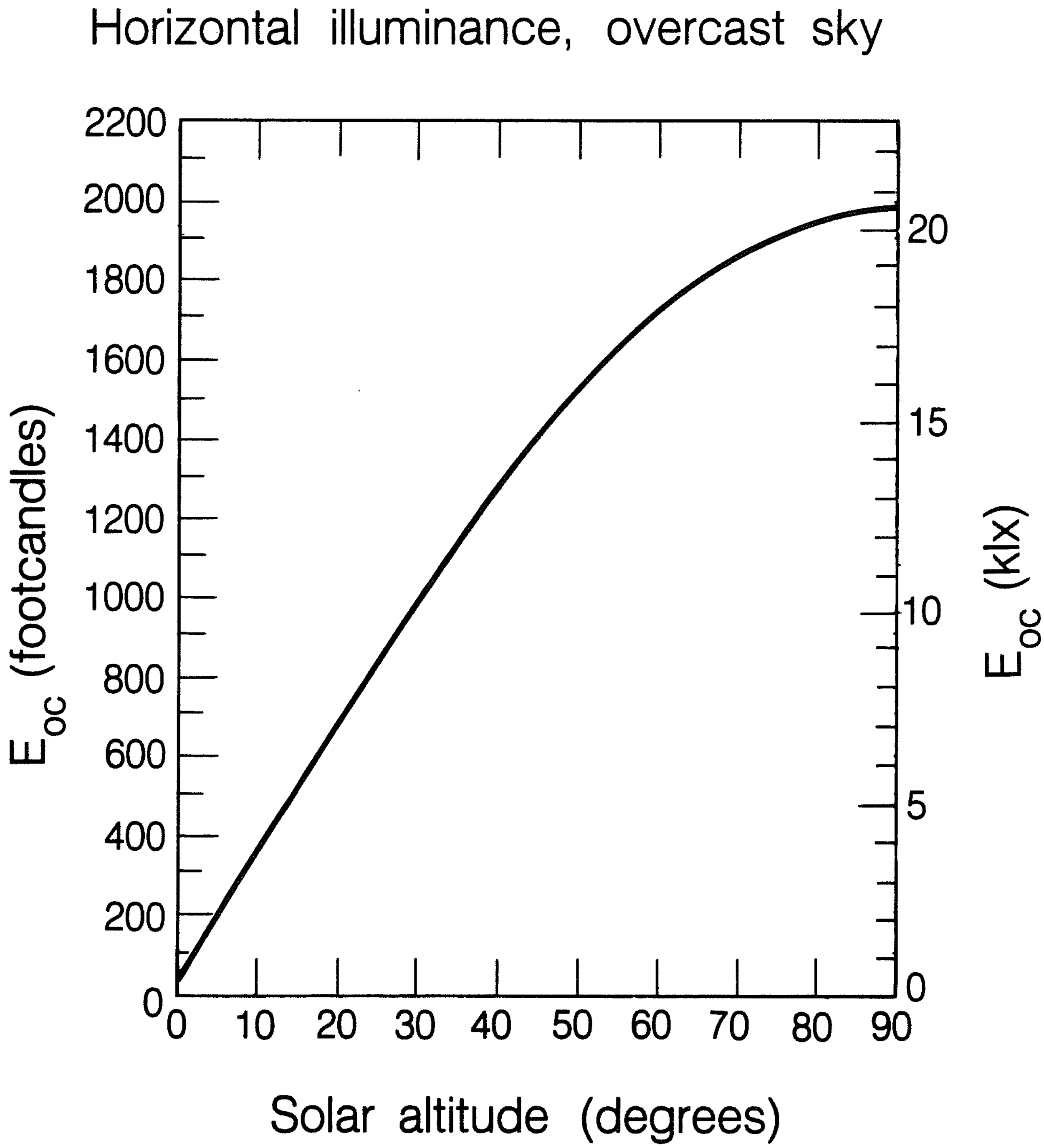

XBL 827-7144

Fig. 5

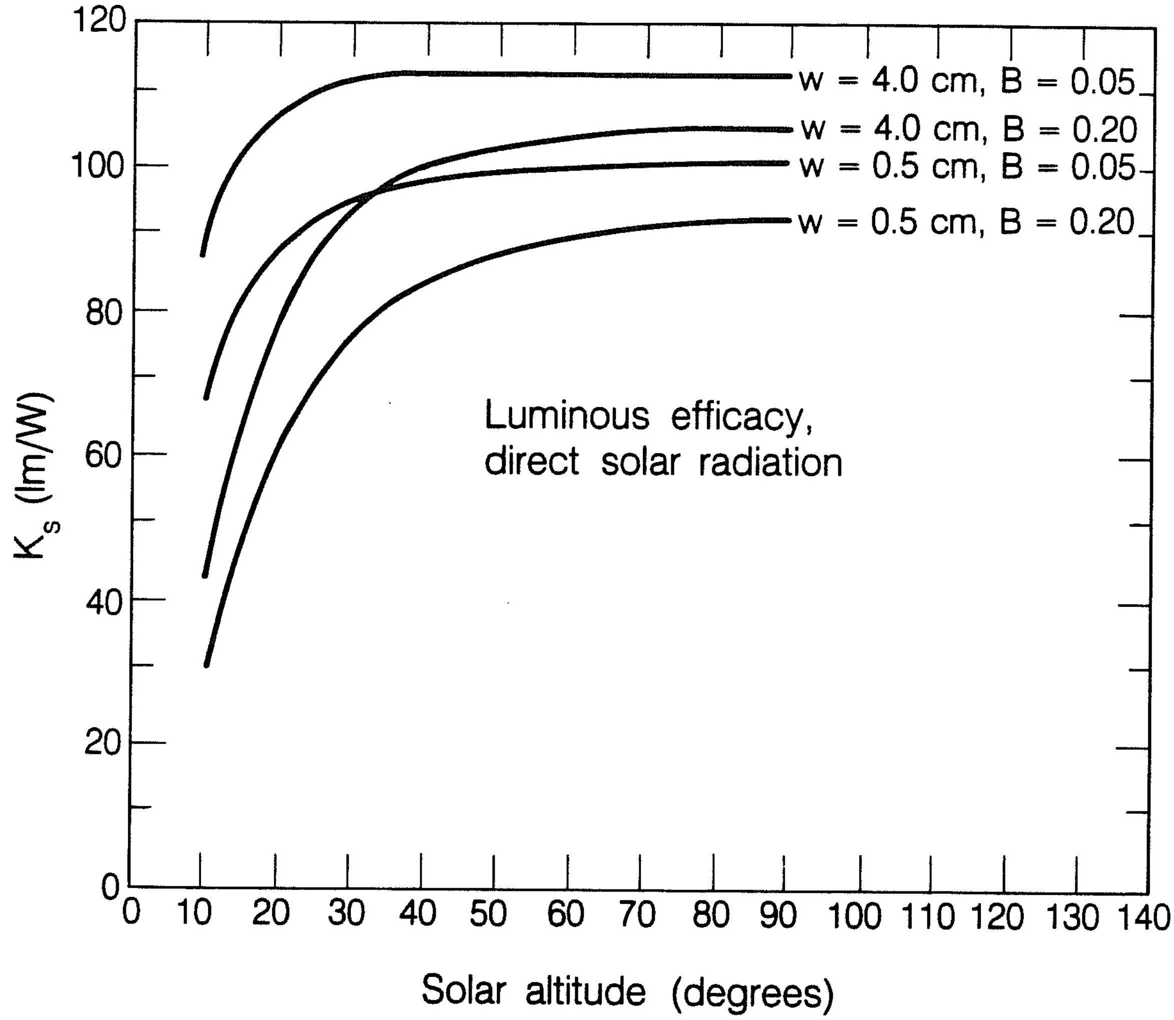

XBL 827-7141

Fig. 6

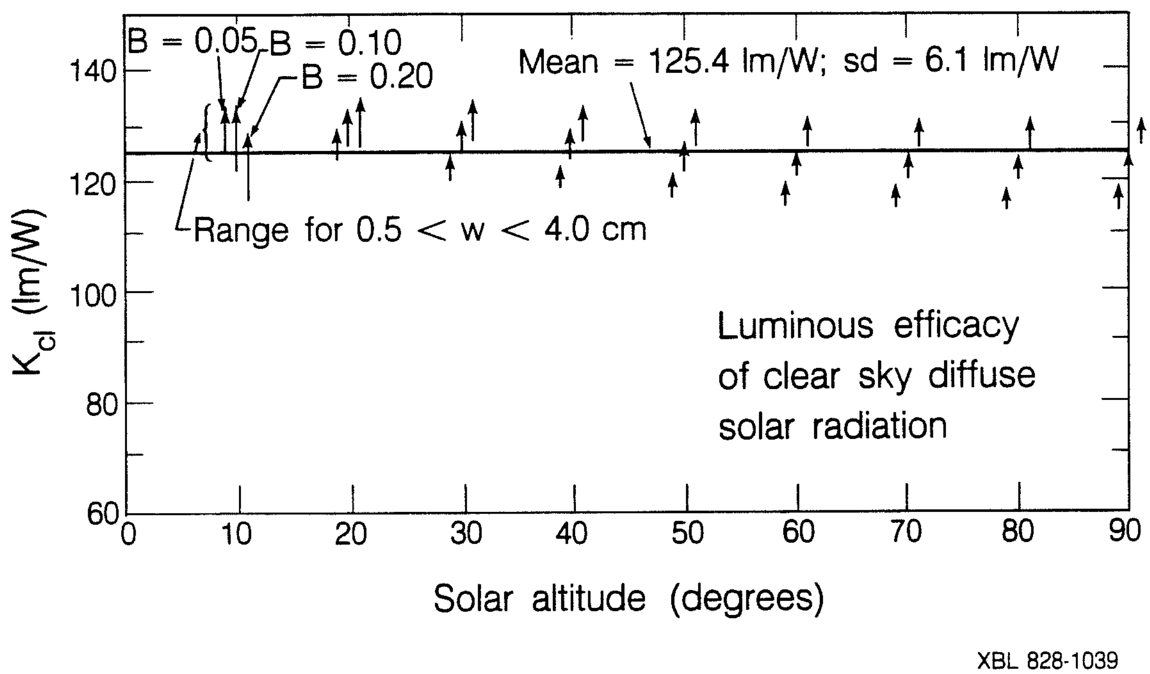
B = 0.05
B = 0.10
B = 0.20
Mean = 125.4 lm/W; sd = 6.1 lm/W
Range for 0.5 < w < 4.0 cm
Luminous efficacy
of clear sky diffuse
solar radiation
K_{cl} (lm/W)
60
80
100
120
140
0
10
20
30
40
50
60
70
80
90
Solar altitude (degrees)
XBL 828-1039

Fig. 7

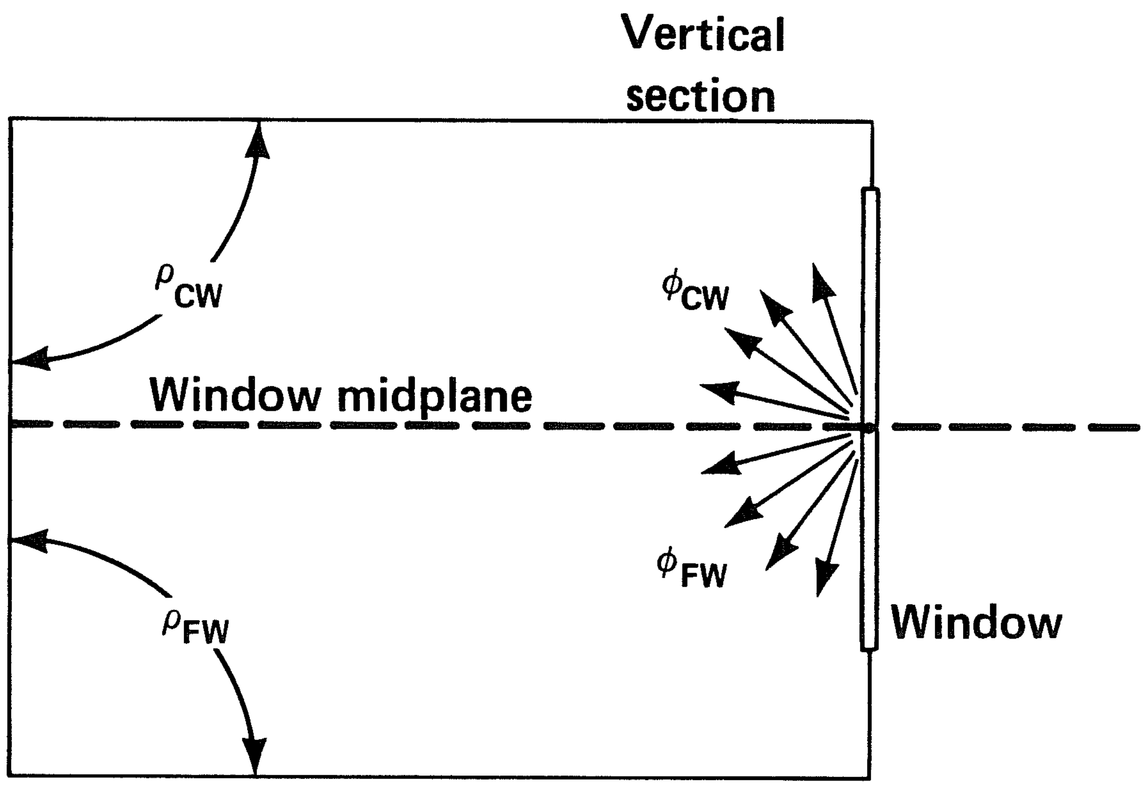

XBL 828 – 1042

Fig. 8

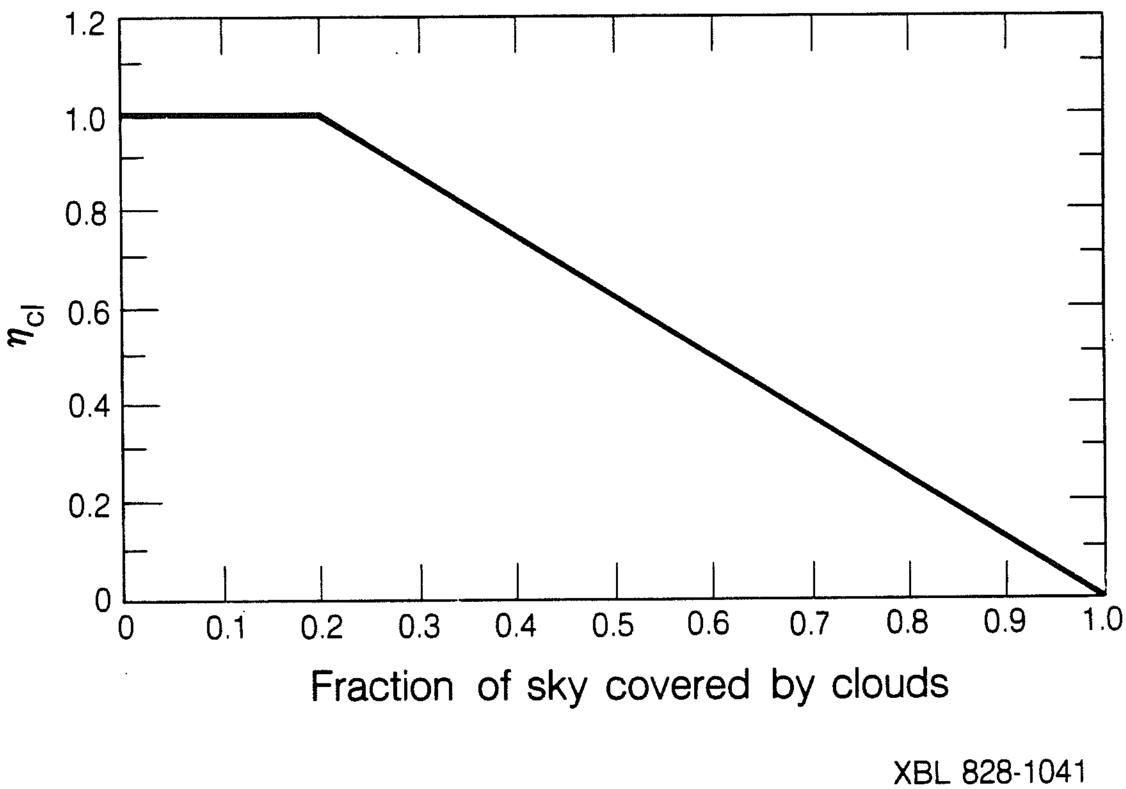
1.2
1.0
0.8
0.6
0.4
0.2
0
η_{cl}
0
0.1
0.2
0.3
0.4
0.5
0.6
0.7
0.8
0.9
1.0
Fraction of sky covered by clouds
XBL 828-1041

Fig. 9

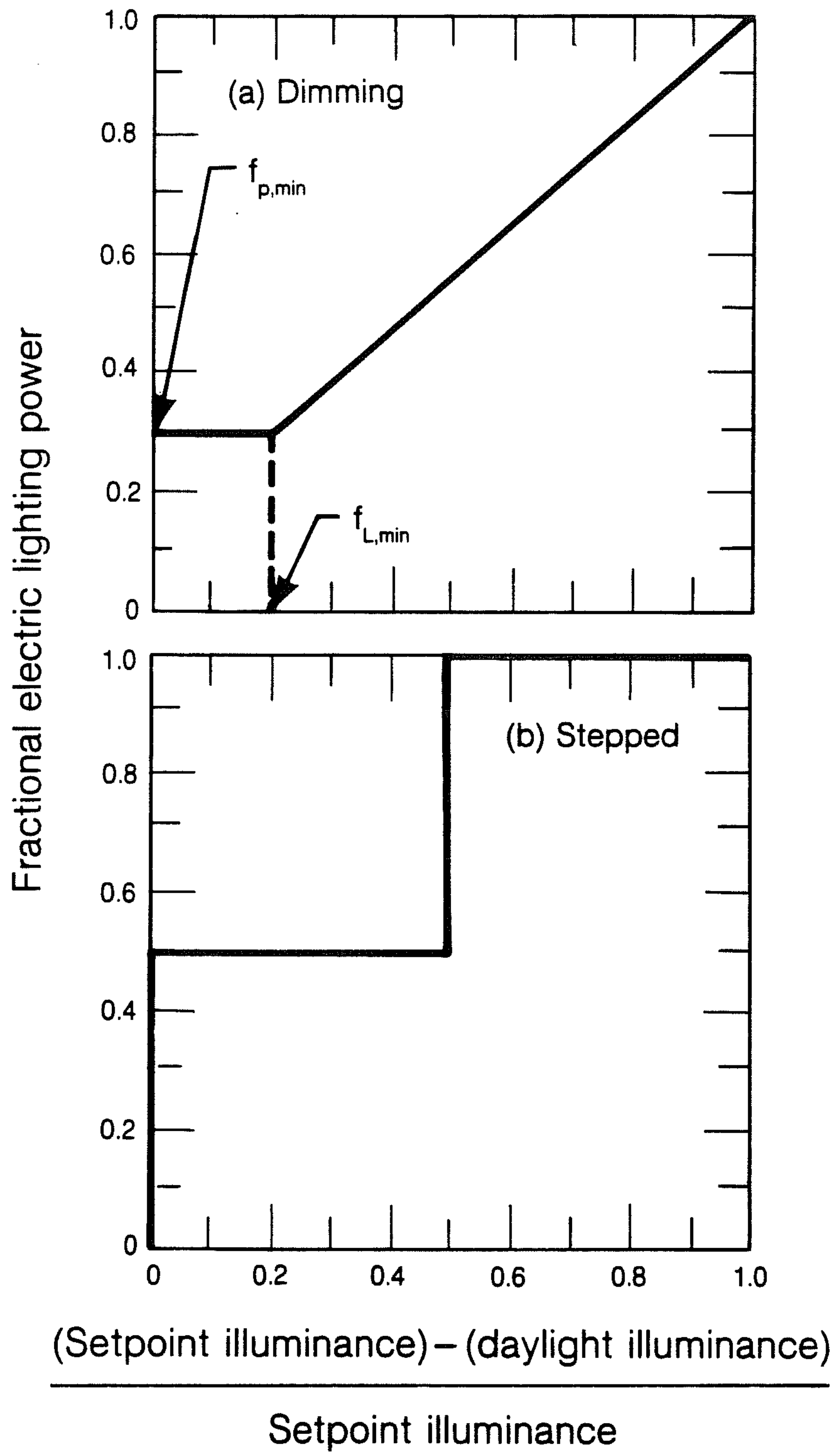

XBL 828-1038

Fig. 10

a

REPORT LS-C SPACE DAYLIGHTING SUMMARY — WEATHER FILE -- MADISON, WI WYEC

SPACE SOUTHZONE

MONTH	PERCENT LIGHTING ENERGY REDUCTION BY DAYLIGHTING (ALL HOURS) TOTAL ZONE	REF PT 1	REF PT 2	PERCENT LIGHTING ENERGY REDUCTION BY DAYLIGHTING (REPORT SCHEDULE HOURS) TOTAL ZONE	REF PT 1	REF PT 2	REPORT SCHEDULE HOURS WITH SUN UP: AVERAGE DAYLIGHT ILLUMINANCE (LUX) REF PT 1	REF PT 2	PERCENT HOURS DAYLIGHT ILLUMINANCE ABOVE SETPOINT REF PT 1	REF PT 2	AVERAGE GLARE INDEX REF PT 1	REF PT 2	PERCENT HOURS GLARE TOO HIGH REF PT 1	REF PT 2
JAN	28.2	34.8	21.7	36.5	45.0	28.0	371.8	173.6	23.7	0.7	19.0	17.2	23.7	17.9
MAR	37.9	45.8	29.9	47.3	56.8	37.8	501.7	241.7	41.2	3.2	20.8	19.4	41.2	30.1
MAY	35.4	46.3	24.4	41.9	54.5	29.3	373.9	183.6	13.6	0.0	20.0	18.6	12.9	1.8
JUL	37.1	48.9	25.2	44.0	57.8	30.2	383.1	188.3	7.9	0.0	20.3	18.9	6.5	0.0
SEP	38.4	47.1	29.7	46.9	57.0	36.7	484.6	237.0	41.5	0.4	20.9	19.7	41.5	28.5
NOV	26.5	33.1	19.8	34.1	42.5	25.6	374.2	173.1	24.8	0.7	18.2	16.5	24.8	21.5
ANNUAL	33.9	42.6	25.1	41.7	52.2	31.3	411.8	198.0	25.9	0.8	19.8	18.3	25.5	16.9

b

REPORT LS-H PERCENT LIGHTING ENERGY REDUCTION BY DAYLIGHT — WEATHER FILE -- MADISON, WI WYEC

SPACE SOUTHZONE

HOUR OF DAY

MONTH	1	2	3	4	5	6	7	8	9	10	11	12	13	14	15	16	17	18	19	20	21	22	23	24	ALL HOURS
JAN	0	0	0	0	0	0	0	3	20	38	47	50	49	50	42	25	10	0	0	0	0	0	0	0	28
MAR	0	0	0	0	0	0	6	24	41	50	47	54	54	50	49	49	32	14	0	0	0	0	0	0	38
MAY	0	0	0	0	0	19	27	35	38	41	44	44	45	47	43	40	32	22	10	0	0	0	0	0	35
JUL	0	0	0	0	0	14	21	29	43	43	45	48	51	50	46	43	28	25	20	1	0	0	0	0	37
SEP	0	0	0	0	0	0	19	34	45	46	51	53	53	51	48	43	32	11	0	0	0	0	0	0	38
NOV	0	0	0	0	0	0	0	12	30	42	47	49	47	42	34	17	2	0	0	0	0	0	0	0	26
ANNUAL	0	0	0	0	0	7	17	29	37	43	47	50	50	47	43	36	20	10	5	0	0	0	0	0	34

c

REPORT LS-J DAYLIGHT ILLUMINANCE FREQUENCY OF OCCURRENCE — WEATHER FILE -- MADISON, WI WYEC

SPACE SOUTHZONE

MONTH	REF PT	PERCENT OF HOURS IN ILLUMINANCE RANGE — ILLUMINANCE RANGE (LUX): 0–100	100–200	200–300	300–400	400–500	500–600	600–700	700–800	800–ABOVE	PERCENT OF HOURS ILLUMINANCE LEVEL EXCEEDED — ILLUMINANCE LEVEL (LUX): 0	100	200	300	400	500	600	700	800
JAN	-1-	13	25	20	10	8	5	3	4	12	100	87	62	42	32	24	18	15	12
	-2-	47	23	12	6	11	1	0	0	0	100	53	30	18	12	1	0	0	0
MAR	-1-	3	15	15	15	11	11	8	9	14	100	97	82	67	52	41	30	22	14
	-2-	23	27	21	16	10	3	0	0	0	100	77	51	29	14	3	0	0	0
MAY	-1-	0	21	15	26	24	12	2	0	0	100	100	79	64	38	14	2	0	0
	-2-	23	42	33	3	0	0	0	0	0	100	77	36	3	0	0	0	0	0
JUL	-1-	0	9	22	30	32	7	1	0	0	100	100	91	69	39	8	1	0	0
	-2-	11	53	34	3	0	0	0	0	0	100	89	37	3	0	0	0	0	0
SEP	-1-	0	18	14	13	14	13	14	9	7	100	100	82	69	55	41	29	15	7
	-2-	23	23	25	23	6	0	0	0	0	100	77	54	29	6	0	0	0	0
NOV	-1-	18	20	17	14	6	3	5	7	10	100	82	62	45	30	25	22	17	10
	-2-	44	25	9	12	9	1	0	0	0	100	56	30	21	10	1	0	0	0
ANNUAL	-1-	6	18	18	18	14	9	6	5	6	100	94	76	58	40	26	17	11	6
	-2-	29	32	21	11	5	1	0	0	0	100	71	39	17	6	1	0	0	0

d

HOURLY-REPORT

MMDDHH	GLOBAL CLOUD AMOUNT	GLOBAL SOLAR ALTITUDE DEGREES	GLOBAL SOLAR AZIMUTH DEGREES	GLOBAL EXT ILL CLR SKY LUX	GLOBAL EXT ILL OVR SKY LUX	SOUTHWIN SHADING FLAG	SOUTHZON DAYL ILL REF PT 1 LUX	SOUTHZON DAYL ILL REF PT 2 LUX	SOUTHZON GLR INDX REF PT 1	SOUTHZON LTPW MUL REF PT 1	SOUTHZON LTPW MUL REF PT 2	SOUTHZON LTPW MUL TOTAL
4 2 6	9.0	1.5	85.0	217.	117.	1.	10.5	3.5	1.3	1.00	1.00	1.00
4 2 7	10.0	8.5	91.6	0.	4752.	1.	93.7	33.9	14.2	0.85	0.94	0.90
4 2 8	10.0	19.3	102.2	0.	11561.	1.	228.0	82.5	18.9	0.63	0.87	0.75
4 2 9	9.0	29.7	114.0	5299.	19784.	2.	201.3	100.1	17.4	0.67	0.84	0.76
4 210	7.0	39.1	128.2	12455.	12851.	2.	478.6	237.7	21.5	0.30	0.61	0.46
4 211	4.0	46.6	145.9	14392.	3322.	2.	665.8	330.5	22.9	0.30	0.46	0.38
4 212	7.0	50.9	167.7	8864.	10618.	2.	695.8	345.3	23.1	0.30	0.44	0.37
4 213	8.0	51.0	191.6	10950.	23623.	2.	541.9	269.9	22.1	0.30	0.56	0.43
4 214	10.0	46.8	213.5	0.	36967.	2.	269.9	134.3	18.9	0.56	0.78	0.67
4 215	10.0	39.4	231.3	0.	11917.	1.	235.0	85.1	19.1	0.62	0.86	0.74
4 216	10.0	30.0	245.6	0.	18205.	1.	362.6	133.6	22.1	0.41	0.78	0.60
4 217	10.0	19.7	257.5	0.	11210.	1.	221.1	80.0	18.8	0.64	0.87	0.76
4 218	10.0	8.8	268.1	0.	2081.	1.	41.0	14.9	9.1	0.93	0.98	0.95

Fig. 11

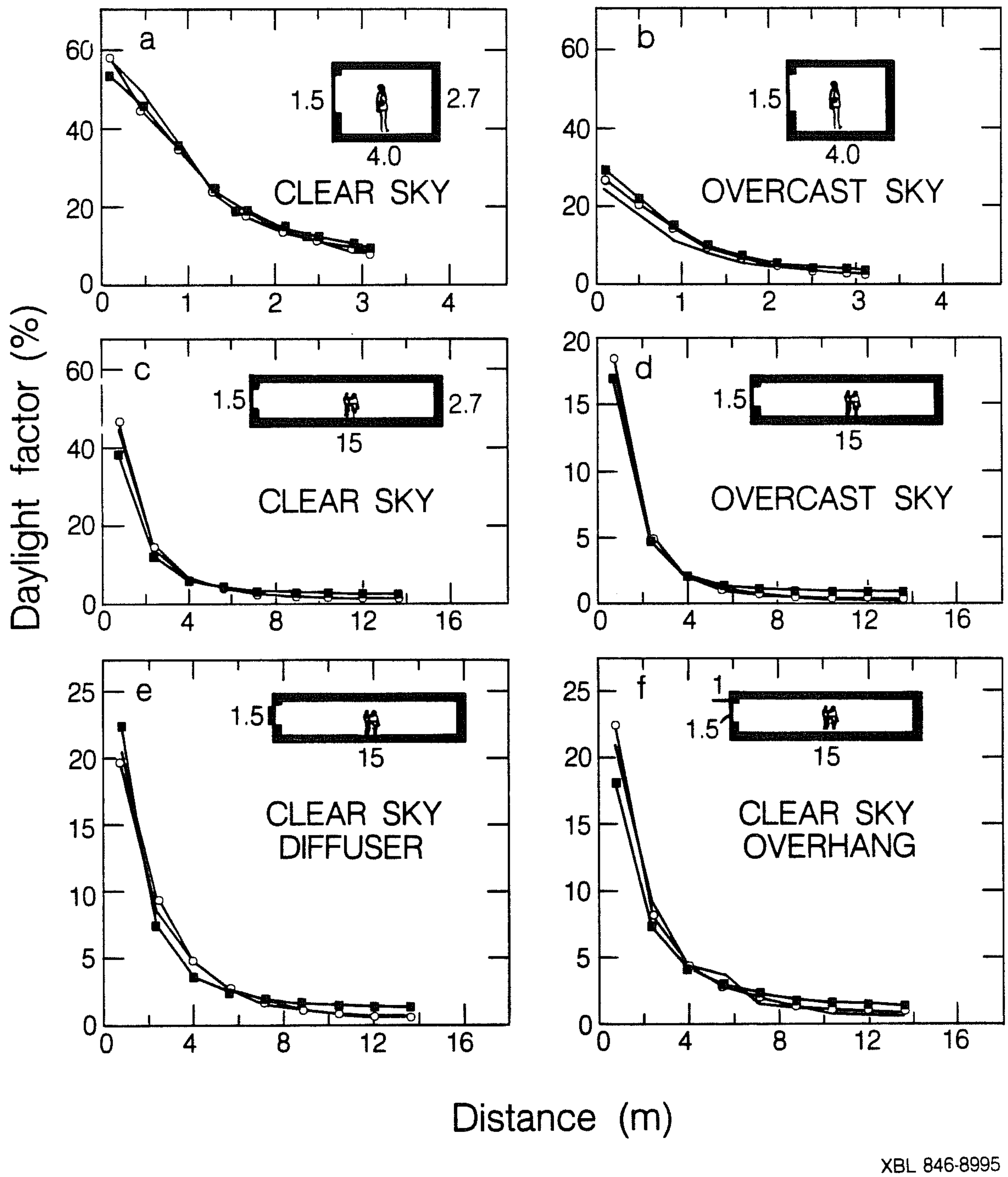
a
1.5
2.7
4.0
CLEAR SKY
b
1.5
4.0
OVERCAST SKY
c
1.5
2.7
15
CLEAR SKY
d
1.5
15
OVERCAST SKY
e
1.5
15
CLEAR SKY
DIFFUSER
f
1
1.5
15
CLEAR SKY
OVERHANG
Daylight factor (%)
Distance (m)
XBL 846-8995

Fig. 12

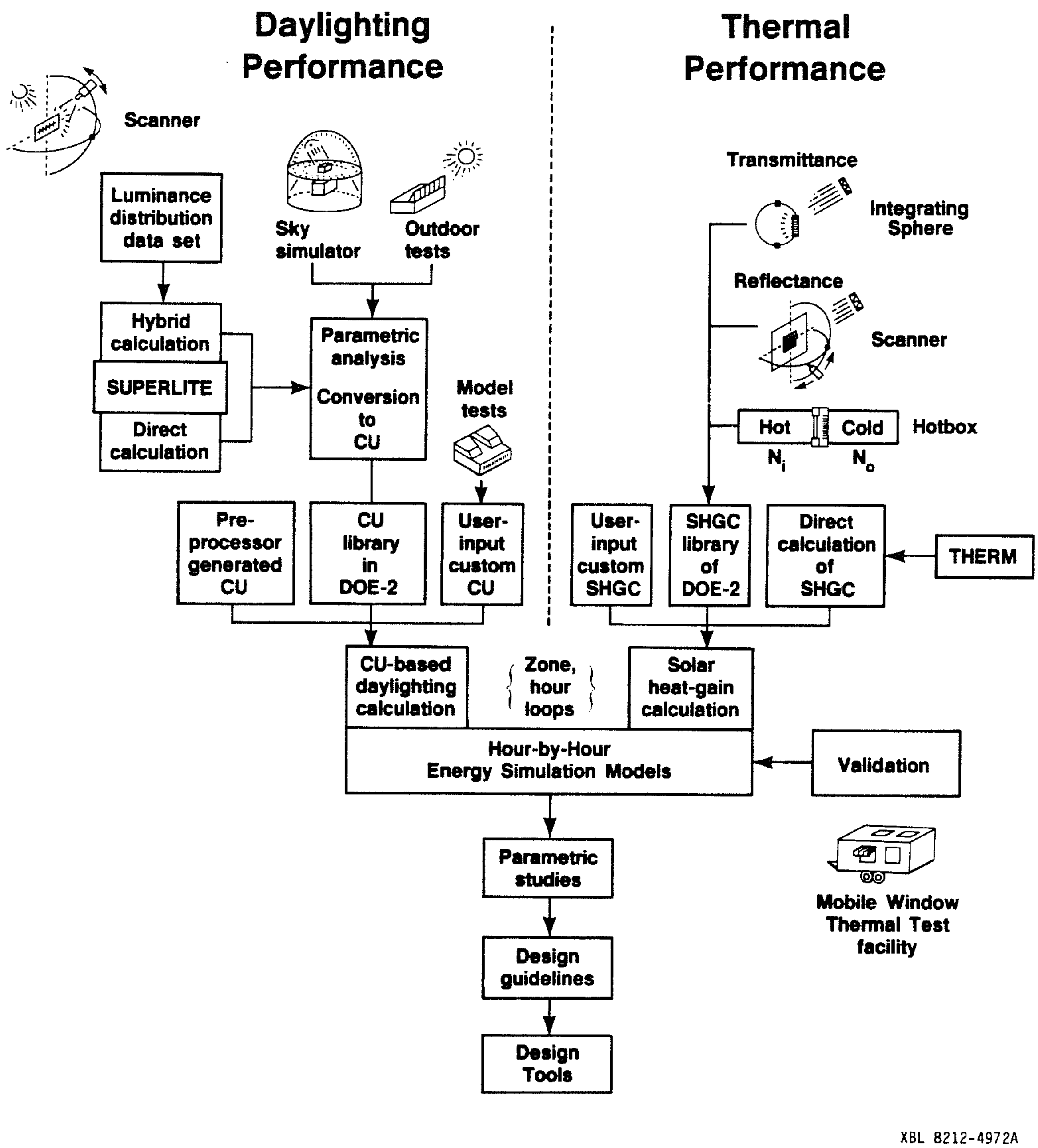
Daylighting Performance
Thermal Performance
Scanner
Luminance distribution data set
Sky simulator
Outdoor tests
Hybrid calculation
SUPERLITE
Direct calculation
Parametric analysis
Conversion to CU
Model tests
Pre-processor generated CU
CU library in DOE-2
User-input custom CU
Transmittance
Integrating Sphere
Reflectance
Scanner
Hot
Cold
Hotbox
N_i
N_o
User-input custom SHGC
SHGC library of DOE-2
Direct calculation of SHGC
THERM
CU-based daylighting calculation
Zone, hour loops
Solar heat-gain calculation
Hour-by-Hour Energy Simulation Models
Validation
Mobile Window Thermal Test facility
Parametric studies
Design guidelines
Design Tools
XBL 8212-4972A

Fig. 13